Title
Insights into Stabilization of the 99TcVO Core for Synthesis of 99TcVO Compounds

Authors
McGregor, Donna
Burton-Pye, Benjamin P.
Lukens, Wayne W.
et al.

Publication Date
2014

Overcoming the synthetic challenges of Technetium-99 polyoxometalates

Or

Oxidation state speciation in the syntheses of Technetium-99 metal oxide complexes: formation of Tc(IV) and Tc(V) polyoxometalates

Benjamin P. Burton-Pye[1], Donna McGregor[1,2], Wayne W. Lukens, Jr.[3], Lynn C. Francesconi[1,2]

[1]Department of Chemistry, Hunter College of the City University of New York

695 Park Avenue, New York, NY 10065

[2] Department of Chemistry, Graduate Center of the City University of New York New York, NY 10016

[3] Chemical Sciences Division, The Glenn T. Seaborg Center, E.O. Lawrence Berkeley National Laboratory (LBNL), One Cyclotron Road, Berkeley, CA 94720

[*]Email: lfrances@hunter.cuny.edu

ABSTRACT

INTRODUCTION

The radioactive element technetium (Tc) possesses 8 oxidation states (-1 to +7). One important isotope, ^{99}Tc (half-life = 2.1 x 10^5 years, β^- of 253 keV), is a major by-product in the nuclear fuel cycle and constitutes ~6 % of the fission yield. ^{99}Tc is also found in radioactive waste tanks from defense activities of the 1940's and 1950's. In some cases due to tank leakage, ^{99}Tc is found in the environment- in water and soils at sites related to the reprocessing of spent nuclear fuel[1-10]. Regardless of the source, separation and storage of the long-lived ^{99}Tc in an appropriate and stable waste-form is an important issue that needs to be addressed.[11]

We are examining the speciation of Tc within metal oxide matrices using polyoxometalates (POMs) as models for metal oxide solid-state materials that may serve as potential storage matrices for Tc. POMs possess surface binding sites as well as "defect" sites with varying electronic and steric properties and "loading capacities". The coordination chemistry and redox speciation can be probed by a number of species-specific techniques to obtain a molecular-level understanding that can be related to solid-state materials. We have found also that POMs can serve to transfer electrons to TcO_4^- to reduce Tc(VII) to lower valent Tc and sequester the low valent Tc[12].

We have employed the well-known phosphorous-tungsten derivatives of the Wells-Dawson polyanion; α-$P_2W_{18}O_{62}^{6-}$, specifically the lacunary derivatives α_1-$P_2W_{17}O_{61}^{10-}$ and α_2-$P_2W_{17}O_{61}^{10-}$. These lacunary ions are achieved through removal of one 'belt' tungsten (a tungsten from one of the two equatorial W_6 rings) or one 'cap' tungsten (a tungsten from one of the two polar W_3 regions) respectively (**Figure 1**). The resulting vacancies provide excellent binding sites for metal ions and have very distinct and different steric and electronic properties.

These properties can be exploited to probe both the coordination and redox properties of metals incorporated into the binding sites. We have reported the Tc and Re complexes of these POMs and compared their stability and chemistry and oxidation reduction behavior. [12-14] Our previous studies include a full detailed synthesis and characterization of $K_{7-n}H_n[Tc^VO(\alpha_1\text{-}P_2W_{17}O_{61})]$ (**Tc^VO-α1**), $K_{7-n}H_n[Tc^VO(\alpha_2\text{-}P_2W_{17}O_{61})]$ (**Tc^VO-α2**), $K_{7-n}H_n[Re^VO(\alpha_1\text{-}P_2W_{17}O_{61})]$ (**Re^VO-α1)** and $K_{7-n}H_n[Re^VO(\alpha_2\text{-}P_2W_{17}O_{61})]$ (**Re^VO-α2)** and full electrochemical comparison.

The combination of a highly redox active metal, such as Tc, with redox-active polyoxometalates creates difficulties in synthesis and isolation of pure complexes. Polyoxometalates are renowned for their ability to accept and transfer electrons to substrates and the **-α1** and **–α2** POMs can accept and transfer multiple electrons.[15-17] In development of the synthesis of the Tc complexes from $Tc^VOCl_4^-$, we observed multiple redox states of the metal ion that presented problems in isolation of pure complexes. We frequently observed Tc(IV) in X-ray Absorption Spectroscopy (XAS) experiments. The important issue and the aim of this study is to identify strategies to minimize hydrolysis and disproportionation of $Tc^VOCl_4^-$ to Tc(IV) and TcO_4^- and to preserve the Tc^VO "core" for incorporation into the POM framework. We also report a strategy using the photocatalytic properties of POMs to reduce TcO_4^- and incorporate the reduced Tc into the POM framework to synthesize Tc POMs in good yield directly from TcO_4^- . In this study, a Tc(IV) partially condensed into the **–α2** POM intermediate is formed that oxidizes to Tc^V that is incorporated fully into the **–α2** framework.

Investigations of these Tc(IV) POM species formed in "traditional" syntheses as well as in the "photoactivated" syntheses leads to the hypothesis that the **–α2** (and **-α1**) POM likely stabilize Tc(IV) preventing the formation of the ubiquitous $TcO_2 \cdot xH_2O$. The rationale and

strategies that we employed to circumvent the formation of Tc(IV) as either $TcO_2 \cdot xH_2O$ or a Tc(IV) μ oxo bridged dimer and to optimize the yield and purity of **$Tc^{V}O$-α1/ α2** in these syntheses may be instructive to others who are interested in isolation of ^{99}Tc complexes either for nuclear energy or environmental applications or to elucidate the structures of ^{99m}Tc radiopharmaceuticals.

EXPERIMENTAL SECTION

General. All materials were purchased as reagent grade and used without further purification. ^{99}Tc is a weak β- emitter with a half-life of 2×10^5 years. All syntheses were performed in a laboratory approved for low-level use of radioactivity using appropriate radioactive material handling procedures. $(NBu_4)TcOCl_4$ was prepared from NH_4TcO_4 according to an established procedure.[18] $K_9Li(\alpha_1\text{-}P_2W_{17}O_{61})$ **(α1)** and $K_{10}(\alpha_2\text{-}P_2W_{17}O_{61})$ **(α2)** ligands were prepared as described in the literature.[19,20] The preparation of $\alpha_1\text{-}[Fe(H_2O)P_2W_{17}O_{61}]^{7-}$ **(Fe-α1)** and $K_{7-n}H_n[Re^{V}O(\alpha_2\text{-}P_2W_{17}O_{61})]$ **($Re^{V}O$-α2)** for electrochemistry were described previously.[19,21] Analytical grade CH_3COONa (Fisher) and glacial CH_3COOH (Acros) were used as received. Pure water used throughout was obtained using a Millipore Direct Q5 system (conductivity =18 μΩ). Infrared analyses were performed on a Perkin Elmer 1625 FTIR Spectrometer.

Synthesis of compounds (optimized and non-optimized):

The optimized syntheses of **$K_{7-n}H_n[Tc^{V}O(\alpha_1\text{-}P_2W_{17}O_{61})]$ ($Tc^{V}O$-α1)**, **$K_{7-n}H_n[Tc^{V}O(\alpha_2\text{-}P_2W_{17}O_{61})]$ ($Tc^{V}O$-α2)**, are similar and were reported previously.[13] Briefly, the syntheses will be summarized below to facilitate the ensuing discussion.

To a 20 mL scintillation vial containing a yellow/green solution of $(NBu)_4TcOCl_4$ (100 mg, 0.2 mmol) dissolved in 1 mL MeOH was added 60 μL (0.98 mmol) of ethylene glycol

$(CH_2OH)_2$ (eg) to produce a blue/green $TcO(eg)_2^-$ complex. This solution was quickly added to a clear, colorless solution of **α1** or **α2** (447 mg, 0.099 mmol) dissolved in 5 mL H_2O (containing LiCl, 10 mg, 0.2 mmol, for the **α1** or at 80°C for **α2**). The resulting dark red solution and brown suspension was stirred for 3 minutes. The reaction mixture was centrifuged (while still warm for **α2**) and the red supernatant decanted. KCl (0.16 g, 2 mmol) was added to the supernatant and was stored at room temperature for up to 48 hours (for the **α1** or 72 hours for **α2**) to allow any unreacted **α1** or **α2** (as monitored by ^{31}P NMR) to precipitate. The mixture was filtered and 10-20 mL of ethanol added to the filtrate to precipitate a dark red solid, which was collected by vacuum filtration. Yields ranged from 40 – 60% based on $(NBu)_4TcOCl_4$. Samples of **Tc^VO-α1** and **Tc^VO-α2** for EXAFS and XANES studies to elucidate oxidation state speciation, were prepared under non-optimal conditions, using less ethylene glycol and precipitation of the product with KCl instead of ethanol. ^{31}P NMR data were collected to monitor the reactions and verify purity.

Experiments to probe the balance between the hydrolysis of the $Tc^VOCl_4^-$ starting reagent and formation of Tc(V) POM were conducted. The amount of the ethyleneglycol transfer ligand and precipitant were varied and all solids were precipitated for XANES analysis. Two stock solutions were prepared by dissolving $K_{10}(\alpha_2\text{-}P_2W_{17}O_{61})$ (700 mg, 0.14 mmol) in 7 mL H_2O and dissolving $TBATcOCl_4$ (100 mg, 0.2 mmol) in dry methanol (2 mL). A 10 µL aliquot of the $TBATcOCl_4$ stock solution was placed in a 2.5 mL vial and the appropriate volume of ethyleneglycol (0, 1.12 or 5.6 µL for 0, 1 and 5 equivalents respectively) was added. After mixing, 100 µL of the $K_{10}(\alpha_2\text{-}P_2W_{17}O_{61})$ stock solution was added, the vial capped and shaken to facilitate mixing. The reaction was allowed to stand for 10 minutes before the addition 2 mL of either a saturated KCl solution or ethanol to initiate precipitation. The solid was collected by

filtration. No recrystallization was performed on these samples. 8 samples were prepared with the composition shown in **Table 1**.

Preparation and Isolation of TcO α2-$P_2W_{17}O_{61}^{7-}$ by photoactivation of α2-$[P_2W_{17}O_{61}]^{10-}$. α2-$[P_2W_{17}O_{61}]^{10-}$ (50 mg, 0.01 mmol) was dissolved in a 2.5 mL mixture of 2:1:1 0.5 M H_2SO_4:2-propanol:D_2O and mixed thoroughly. This resulted in 4 mM POM solution. The solution was placed in a quartz luminescence cuvette. Standardized TcO_4^- (0.28 M) was added (50 μL, 14 mmol) and the cuvette was sealed with a rubber septum and purged with N_2 for 30 min before irradiation with a UV lamp at 254 nm (power @ 5 cm from source = 17.9 @ 200 μW) for 24 hours. After the irradiation periods, the colorless solution changed to dark red. A saturated KCl solution (500 μL) was added directly to the reaction solution. The reaction was placed in the refrigerator overnight and the dark red crystals that formed were collected by filtration (49 mg, 0.009 mmol). Alternately the saturated solution of KCl can be replaced by a TBABr solution (10 mg in 500 μL) to initiate immediate precipitation of the TBA salt of **TcO α2-$P_2W_{17}O_{61}$.** This precipitate contains small amounts of $TBATcO_4$ that can be removed by washing the filtrate with ethanol (x mg, x mmol). Yields:

Collection of NMR Data. NMR data were collected on a JEOL GX-400 spectrometer with 5 or 10 mm tubes fitted with Teflon insert that were purchased from Wilmad Glass. Resonance frequencies are 161.8 MHz for ^{31}P. Chemical shifts are given with respect to external 85% H_3PO_4 for ^{31}P. Typical acquisition parameters for ^{31}P spectra included the following: spectral width, 10000 Hz; acquisition time, 0.8 s; pulse delay, 1 s; pulse width, 15 μs (50° tip angle). From 200 to 1000 scans were required. The temperature was controlled to ± 0.2 deg. For the ^{31}P chemical shifts, the convention used is that the more negative chemical shifts denote more upfield resonances.

Collection of X-ray Absorption Spectroscopy Data: XAS data on non-optimized syntheses of **$Tc^{V}O$-α1** and **$Tc^{V}O$-α2** were collected on two occasions. One set (EXAFS and XANES) was collected in 2009 to probe coordination environment and redox speciation and a second set (XANES) was collected in April, 2011 in experiments designed to probe the synthesis conditions leading to speciation.

Experimental Conditions in 2009 on non-optimized synthesis of* $Tc^{V}O$-α1 and $Tc^{V}O$-α2*: Both EXAFS and XANES experiments were performed on the non-optimized syntheses. Samples were dissolved in 1 mL of 18 MΩ water then transferred to 2 mL screw capped centrifuge tubes. Transmission data was acquired at SSRL beamline 4-1. Harmonic content of the beam was reduced by detuning the monochromator by 50%. The data was processed using EXAFSPAK and Athena/ifeffit.[22,23] Data was fit using Artemis/ifeffit and theoretical phases and amplitudes calculated using FEFF7.[24] The initial model used in the FEFF calculation was $(NH_4)_6(P_2W_{18}O_{62})$ with one W atom replaced by Tc.[25] Additional scattering shells were added only if their inclusion lowered the value of reduced chi squared.

The F-test was used to analyze the significance of the fitting parameters including the significance of adding a scattering shell.[26] The null hypothesis is that the additional shell of atoms does not improve the fit. The result of the F-test is the probability, p, that this hypothesis is correct. If $p < 0.05$, the null hypothesis is rejected in favor of the alternative hypothesis that the additional shell significantly improves the fit. [27]

Sample preparation in April 2011: In this set of experiments, samples of **$Tc^{V}O$-α2** were prepared as a function of amount of ethyleneglycol and varying the precipitant. All precipitated solid was collected and examined by XANES to identify oxidation states of the Tc products and percentages of Tc^{IV}, Tc^{V}, and Tc^{VII}.

Samples were dissolved in 1 mL DI water, shaken vigorously then solicited for ~ 1 minute. Samples were allowed to sit overnight then were separated by centrifugation. The solution phase was carefully decanted from the solid phase and placed in 2 mL screw top polypropylene centrifuge tubes, which were decontaminated and further contained in two heat-sealed plastic pouches.

Data were collected SSRL BL 11-2 in fluorescence using a 30 element Ge detector and in transmission using Ar-filled ion chambers. Fluorescence data were corrected for detector dead time. Data were worked up using Athena.

Three reference spectra were used, TcO_4^- (the reference sample recorded during this beamtime), Tc^V=O in alpha-2 WD ion, and $TcO_2 \bullet 2H_2O$ (the $TcO_2 \bullet 2H_2O$ data were convolved with a 2 eV Gaussian to better match the data.). Data were fit using the local code 'fites.' When possible, transmission data was used; however, for two samples, 11 Eg E and 115E, the quality of the transmission data was much poorer than the fluorescence data, so the fluorescence data was used instead.

RESULTS AND DISCUSSION

^{31}P NMR to monitor speciation: ^{31}P NMR is very useful to monitor speciation of these complexes. Typical ^{31}P NMR data are shown in **Figure 2**. Both the **Tc^VO-α1** and **Tc^VO-α2** species possess two phosphorous atoms: one close and one remote from the site of substitution. Therefore, two resonances are expected for pure complexes. Chemical shifts for the **Tc^VO-α1** and **Tc^VO-α2** species, unbound **-α1** and **-α2** ligands, and intermediate species have been published.[12,13]

Synthetic Challenges of $Tc^{V}O$-α1 and $Tc^{V}O$-α2 complexes: The synthesis of pure transition metal polyoxometalates is often complicated by the difficulty in separating unreacted POM ligand from the metal POM complex. Usually separations are achieved by fractional crystallizations and are complicated by the similar solubilities of the metal complexes of POMs and the POM ligands. Separations are rendered even more difficult due to the small volumes manipulated in fractional crystallizations when working with milligram quantities of ^{99}Tc. The small volumes, multiple oxidation states accessible to ^{99}Tc, and hydrolysis of the $^{99}TcOCl_4^-$ starting reagent generally compromise separation of reactant from products, reproducibility and yield of the reactions

The $(NBu_4)TcOCl_4$ starting reagent readily hydrolyzes and subsequently disproportionates in water and in methanol forming $TcO_2 \bullet xH_2O$ and TcO_4^- To stabilize this source of $Tc^{V}O$, $(NBu_4)TcOCl_4$ was treated with ethylene glycol, which acts as a "transfer ligand" to inhibit hydrolysis of $Tc^{V}O$ and facilitate its transfer to the **-α1** and **-α2** ligands. Transfer ligands are routinely used in radiopharmaceutical applications with the tracer ^{99m}Tc to stabilize the $^{99m}Tc^{V}$=O core for ligand substitution with a stronger ligand. The $TcO(eg)_2^-$ transfer complex[28,29] is formed *in situ,* and the ethylene glycol ligands are replaced by the tetradentate **α1/α2** ligands to form the Tc^{V} complexes. This is shown schematically in **Figure 3**.

If too little ethylene glycol is used to stabilize Tc(V), hydrolysis of the $TcOCl_4^-$ starting material to $TcO_2 \bullet H_2O$ occurs, *vide infra*, resulting in inconsistencies in the ^{31}P NMR data used to monitor the progress of the reaction. The ^{31}P NMR resonances are often paramagnetically broadened or not visible due to the presence of $TcO_2 \bullet xH_2O$. $TcO_2 \bullet xH_2O$ is typically colloidal and often cannot be filtered from the reaction solution. **Table 2** presents the ^{31}P NMR data for the stages of one such reaction.

In general, the crude reaction mix showed no peaks in the ^{31}P NMR (due to the presence of the paramagnetic $TcO_2 \bullet xH_2O$ species). The colloidal $TcO_2 \bullet xH_2O$ was removed from the crude reaction mixture by centrifugation for 15 minutes at 7,000 rpm. The supernatant showed peaks of the desired product as well as excess **α1/α2** starting material. Allowing the supernatant to stand at room temperature overnight resulted in the precipitation of a mixture of white and black-brown material. The white solid was identified as the **α1** or **α2** ligand (by ^{31}P NMR), and the black-brown solid was postulated as a mixture of $TcO_2 \bullet xH_2O$ and **Tc^{V}O-α1** or **Tc^{V}O-α2** as a tetrabutylammonium salt (soluble in acetonitrile and identified by ^{31}P NMR).

After filtering to remove the solids, the dark red filtrate showed ^{31}P NMR peaks of pure product (**Table 2** shows this for **Tc^{V}O-α2**), further affirming that the white solid was indeed unreacted ligand. If the original supernatant was allowed to stand for periods more than one week $(\alpha\text{-}P_2W_{18}O_{62})^{6-}$,the parent Wells-Dawson POM, formed in solution. This $(\alpha\text{-}P_2W_{18}O_{62})^{6-}$ was consistently difficult to separate from the desired product.

Isolation of solid product was initially attempted by adding an excess of KCl. Although this did result in the formation of a dark brown solid, once dissolved, this solid showed no identifiable product peaks in the ^{31}P NMR. In subsequent reactions, it was discovered that the use of a minor amount of KCl (to aid the precipitation of impurities and excess ligand), followed by the addition of an excess of ethanol resulted in the isolation of pure **Tc^{V}O-α1** or **Tc^{V}O-α2**, as identified by ^{31}P NMR. The yields obtained for these reactions were never more than 60 %. The low yields are primarily attributed to the formation of $TcO_2 \bullet xH_2O$. It was found that maintaining a 1:1 ratio of Tc to **α1** or **α2** is important for optimizing both the yield and purity of the product.

Even a small excess of Tc (>1 eq.) results in the formation of a large amount of dark brown/black precipitate (presumed to be $TcO_2 \bullet xH_2O$). Using an excess of **α1** or **α2** to compensate for this does not prevent formation of $TcO_2 \bullet xH_2O$; rather, the result is always an excess of **α1** or **α2** present in the crude product (as determined by ^{31}P NMR). This phenomenon would indicate that the formation kinetics of **$Tc^{V}O$-α1** or **$Tc^{V}O$-α2** are slower than that of the disproportionation of Tc(V) to $TcO_2 \bullet xH_2O$.

The use of ethylene glycol as a transfer ligand to inhibit the hydrolysis of $TcOCl_4^-$ and facilitate transfer of Tc for isolation of **$Tc^{V}O$-α1** and **$Tc^{V}O$-α2** proved successful. The $TcO(eg)_2^-$ complex[28] was not isolated during the procedure, but rather formed *in situ.* When **α1/α2** is added to this $TcO(eg)_2^-$ transfer complex, the ethylene glycol ligands are replaced by the tetradentate **α1/α2** to form **$Tc^{V}O$-α1/α2**.

In addition to the 1:1 Tc: **α1** and **α2** stoichiometry, we found that a Tc:eg ratio of between a 1:3.5 and 1:6 was required to obtain an optimal yield and purity.[13] A ratio of less than 1:3.5 resulted in the formation of an increased amount of both the containing dark solid (presumably $TcO_2 \bullet xH_2O$) and free **α1** or **α2**, ligand, while a ratio of more than 1:6 resulted in a low yield and increased difficulty when isolating a pure product as a solid. It should be noted however, that upon scale-up of the reaction an increased ratio of eg:Tc became necessary to stabilize the $Tc^{V}O$ core against disproportionation to $TcO_2 \bullet H_2O$.

Extended X-ray absorption fine structure (EXAFS) spectra of the products of non-optimized syntheses of **$Tc^{V}O$-α1** and **$Tc^{V}O$-α2** showed carryover of Tc(IV) from the hydrolysis of the $Tc^{V}O$ starting material into the product, vide infra. A significant fraction of Tc^{IV} was found in **$Tc^{V}O$-α1** and **$Tc^{V}O$-α2** complexes that were produced using too little ethylene glycol to stabilize the $Tc^{V}O$ reagent. This result will be discussed below in the XAS section, below.

X-ray absorption fine structure.

XAS on optimized syntheses (published):

The XAS on the optimized syntheses have been published.[13] We will summarize the findings here.

$Tc^{V}O$-α2: The local structure obtained by fitting EXAFS spectrum of **$Tc^{V}O$-α2** complexes is consistent with the structure of the cap W site of the Wells-Dawson ion. The oxygen coordination environment contains a very short Tc-O bond, 1.64 Å, which is consistent with the terminal oxo ligand of a Tc(V) ion, and the best fit is obtained with 4 oxygen ligands at 2.00 Å and a more distant oxygen neighbor at 2.53 Å.

$Tc^{V}O$-α1: The EXAFS data revealed that the **$Tc^{V}O$-α1** possesses the short Tc-O bond, 1.64 Å, typical of Tc(V) but has 5 next-nearest oxygen neighbors at 1.97 Å, rather than the 4 next-nearest oxygen neighbors found in **$Tc^{V}O$-α2**. Overall, the data suggest that the Tc(V) center in **$Tc^{V}O$-α1** has been "pulled into" the Wells-Dawson ion relative to the position of the belt W atom.

XAS data for non-optimized syntheses of $Tc^{V}O$-α1 and $Tc^{V}O$-α2 :

Complexes of **$Tc^{V}O$-α1** and **$Tc^{V}O$-α2** that were produced using too little ethylene glycol ("non-optimized" syntheses) were also analyzed by XANES (**Figure 4**) and EXAFS (**Figure 5**, **Tables 3**, **4** and **5**). EXAFS analysis taken on **$Tc^{V}O$-α1** and **$Tc^{V}O$-α2**, produced by "non-optimized" syntheses, showed the presence of an additional Tc atom at 2.53 – 2.57 Å. The model used to fit the data included either a terminal oxo ligand at 1.75 Å for the Tc(V) species or a Tc atom at 2.55 Å for the Tc(IV) species. Inclusion of theTc atom at 2.55 Å significantly improved the fit ($p < 0.007$). The Debye-Waller parameter of this Tc neighbor is fixed at a reasonable value (0.003 $Å^2$) to allow the relative amount of Tc in different samples to be

compared. Fixing the Debye-Waller parameter in this manner means that the absolute proportion of Tc(IV) in the sample cannot be quantified because the Debye-Waller parameter is strongly correlated with the number of neighboring atoms.

The origin of this Tc(IV) contribution is likely hydrolysis and disproportionation of the $Tc^{V}OCl_4^-$ starting reagent. The Tc at 2.53-2.57 Å could be due to either reduction of the Tc(V) complex to Tc(IV) followed by dimerization to the Tc^{IV}-(μ-$O)_2$-Tc^{IV} **α1/α2** dimer, or to a Tc^{IV}-(μ-$O)_2$-Tc^{IV} ethyleneglycol complex. Alternatively, the Tc(IV) could be due to a colloidal TcO_2•xH_2O impurity. Comparison of these models show that neither is significantly better (p = 1.0). However, the results given in **Table 3** and **Table 4** (corresponding to data in **Figures 5a**, and **5b** (data collected two months later)) strongly suggest that Tc(IV) is not present as TcO_2•xH_2O. **Figures 5a** and **5b** of **Tc^{V}O-α1** show almost identical spectra, and **Tables 3** and **4** reveal almost identical fit parameters, which suggest that the Tc(IV) present in the sample is resistant to oxidation by atmospheric oxygen. This behavior is not consistent with TcO_2•xH_2O, which is readily oxidized by oxygen.[1-4,8,30,31] The amount of Tc(IV) in the **Tc^{V}O-α1** sample is significantly greater than in the **Tc^{V}O-α2** sample, but in both cases, the major portion of the technetium is present as a Tc(V) complex as suggested by the XANES data (**Figure 4**).

EXAFS, XANES and multinuclear NMR experiments from a study published recently where the **-α2** ligand was employed for photoactivation and reduction of TcO_4^- demonstrated that a Tc(IV) **-α2** intermediate species is formed. This intermediate oxidizes to Tc^{V} and incorporates into the framework forming the **Tc^{V}O-α2** product. These studies clearly point to the stability of Tc(IV) adducts of **α1/ α2** ligands and argue that the Tc^{IV}-(μ-$O)_2$-Tc^{IV} dimer contains **α1/ α2** ligands. Electrochemical studies (manuscript under review) on the **Tc^{V}O-α1** and **Tc^{V}O-α2**

complexes where the TcV → Tc(IV) reduction processes are reversible also argue that Tc(IV) **-α1/ α2** complexes are stable.

After demonstrating that Tc^{IV}-$(\mu\text{-}O)_2$-Tc^{IV} product and **Tc^{V}O-α1/ α2** species were present in the preparations, we carried out studies to correlate the amount of these species (**Tc^{V}O-α2**, Tc^{IV}-$(\mu\text{-}O)_2$-Tc^{IV} product, TcO_4^-) with the amount of ethylene glycol and the precipitant used in the preparations. Samples were prepared varying the $TcOCl_4^-$/eg ratio, and using KCl or ethanol as precipitants; in one experiment $TcO(eg)_2^-$ was used as the Tc source. **Table 1** shows the composition of the samples. **Figure 6** shows the XANES experiments for samples 115K and 115E . **Figures S1**-**S6** show the XANES experiments for the rest of the samples.

Table 6 and **Figure 7** contain the speciation information for the samples as determined by fitting the XANES spectra. **Table S1** contains the fitting parameters. In general, the fits modeled the data well with the exception of sample 11 Eg E. For this sample, the fit is quite poor that it is unlikely that any of the component spectra (TcO_4^-, **Tc^{V}O-α2**, or TcO_2•$2H_2O$) represents the local environment of Tc in this compound. For the rest of the samples, the data were well modeled by the 3 component spectra. It should be noted that the TcO_2•$2H_2O$ standard is a substitute for the Tc^{IV}-$(\mu\text{-}O)_2$-Tc^{IV} product found in the above EXAFS experiments. It is unlikely that the XANES spectrum of Tc(IV) coordinated by the lacunary **-α2** ion occurs at a different energy than that of TcO_2•$2H_2O$. In addition, TcO_2•$2H_2O$ is sensitive to oxidation by atmospheric oxygen under the conditions present in these samples and should have oxidized to TcO_4^- by the time the spectra were obtained.

Many of these samples contained a large amount of TcO_4^-. There are two possible sources of this ion. First, it may have been produced directly by disproportion of the Tc(V) ; the Tc(IV)

would be incorporated into the into the **α1/ α2** frameworks. Another source of TcO_4^- could be oxidation of $TcO_2 \bullet xH_2O$.

The XANES analysis shown in **Table 6** demonstrates that the reaction of the $TcO(eg)_2^-$ complex with the **α2** ligand results in only 10% **Tc^VO-α2** and 60% TcO_2 or Tc^{IV}-$(\mu\text{-}O)_2$-Tc^{IV} product (see above) and 25% TcO_4^-. All samples prepared with 1:1 **α2**:$TcOCl_4^-$ show at least 50% of the **Tc^VO-α2** product. Adding ethylene glycol significantly increases the amount of the **Tc^VO-α2** product. However, in these experiments, there were no significant differences in the **Tc^VO-α2** product yield with 1 equivalent of eg or 5 equivalents of eg.

In all cases, we see a significant amount of TcO_2 by-product. As mentioned above, this Tc(IV) by-product is likely a Tc^{IV}-$(\mu\text{-}O)_2$-Tc^{IV} dimer of the **-α2** ligand. We see reversible $Tc^{V/IV}$ redox processes in the cyclic voltammograms of the **Tc^VO-α1/ α2** leading us to conclude that these species are stable. Also, using the **α2** ligand for photoactivation and reduction of TcO_4^-, we observe by EXAFS and XANES a Tc(IV) **α2** "intermediate" species that slowly oxidizes to Tc^V and incorporates into the framework forming the **Tc^VO-α2** product.[12] These studies clearly point to the stability of Tc(IV) adducts of **α1/ α2** ligands.

Preparation and Isolation of TcO α2-$P_2W_{17}O_{61}^{7-}$ by photoactivation of α2-$[P_2W_{17}O_{61}]^{10-}$

Photocatalytic reduction of organic materials and metal ions to metallic nanoparticles can be accomplished using plenary POMs. [33-45] These plenary POMs can be reduced by multiple electrons while maintaining their structural integrity and act as cathodes to efficiently transfer electrons to the organic material or metal. The re-oxidized plenary ion thus stabilizes the reduced organic material or metal nanoparticle by electrostatic surface interactions.[33,40,43,44,46,47] We have found that the plenary Keggin ions $(PW_{12}O_{40})^{3-}$, $(SiW_{12}O_{40})^{4-}$ and $(AlW_{12}O_{40})^{5-}$ photocatalytically reduce TcO_4^- to low valent Tc (Tc^{IV}) and stabilize it.[12]

In a previous study[12], we found that the lacunary **α2** can be photoactivated for reduction of TcO_4^- (and ReO_4^-) and the reduced metal can be incorporated into the defect binding site. **Figure 8** describes the process: the **α2** ligand accepts 2 electrons from a sacrificial electron donor (isopropanol) and transfers these electrons to TcO_4^- for reduction to a Tc^{IV}-**α2** intermediate that slowly and quantitatively oxidizes to Tc^V. Moreover, the re-oxidized **α2** can quantitatively incorporate the generated Tc^V (and Re^V) covalently into the framework via bonding to the four basic oxygen atoms that comprise the **α2** defect site. This can be accomplished in a "one-pot" reaction, which spurred us to implement this process as a synthetic tool.

A solution containing 4 mM POM and 14 mM TcO_4^- and (how much?)H_2SO_4 and isopropanol was placed in a quartz luminescence cuvette and purged with N_2 for 30 min before irradiation with a UV lamp for 24 hours. During the irradiation period, the colorless solution changed to dark red. ^{31}P NMR taken during the process shows the **TcO-α2** product along with the Tc^{IV}-**α2** intermediate that converts to the product with time. The product can be isolated in good yield by adding KCl solution directly to the reaction solution and cooling the solution to form dark red crystals. The excess of TcO_4^- in the reaction insures that the **α2** POM will be

used up in the reaction and thus the addition of KCl results in crystallization of pure K **TcO-α2** product.

To isolate an organic soluble **TcO-α2**, Tetrabutylammonium bromide ($N(C_4H_9)_4Br$, TBABr) was added to precipitate the TBA salt of **TcO-α2**. This precipitate contains small amounts of $TBATcO_4$ that can be removed by washing the filtrate with ethanol. The ^{31}P NMR data for the K^+ salt is identical to that shown in **Figure 8**. The ^{31}P NMR of the TBA salt is shown in **Figure 9**. Describe/discuss the NMR. This photosynthetic strategy for the formation of TBA salts of the POMs is convenient and straightforward. On the other hand, for formation of TBA complexes of metal **-α2**, generally requires metathesis from the aqueous salts. [48]

The use of POMs for photocatalytic or photoactivated preparation of aqueous and organic soluble Technetium-99 materials is a new and straightforward synthetic strategy. This strategy demonstrates the value of working with redox active ligands in combination with Technetium.

CONCLUSION

ACKNOWLEDGEMENT

We are grateful to the NSF (Grant Nos. CHE 0414218 and CHE 0750118), the Office of Science (BER)- U.S. Department of Energy (DOE) (Award DE-SC0002456), and to DE-FG02-09ER16097 (Heavy Element Chemistry, Office of Science, Department of Energy) for support of this work. We are grateful to NSF-CHE 0959617 for the purchase of the 400 MHz NMR used in this research. Research infrastructure at Hunter College is partially supported by Grant Number RR003037 from the National Center for Research Resources (NCRR), a component of the

National Institutes of Health (NIH). Part of this work was performed at Lawrence Berkeley National Laboratory and was also supported by Heavy Element Chemistry, Office of Science, Office of Basic Energy Sciences of the U.S. Department of Energy (DOE) under Contract No. DE-AC02-05CH11231. EXAFS data were obtained at the Stanford Synchrotron Radiation Laboratory, a national user facility operated by Stanford University on behalf of the U.S. DOE, Office of Basic Energy Sciences.

Figure Captions:

Figure 1.

Figure 2. ^{31}P NMR of $Tc^{V}O$-α1 and **$Tc^{V}O$-α2**

Figure 3. Scheme showing fate of $TcOCl_4^-$ upon hydrolysis to Tc(IV) and upon application of ethyleneglycol as a transfer ligand to preserve the Tc^{V}=O core for substitution with the POM.

Figure 4. XANES spectra of, from lowest energy to highest energy, TcO_2•$2H_2O$ (blue), **$Tc^{V}O$-α2** (red), **$Tc^{V}O$-α1** (black), and TcO_4^- (green). The **$Tc^{V}O$-α1** and **$Tc^{V}O$-α2** samples are from the non-optimized syntheses, where the carryover of the Tc^{IV}-$(\mu\text{-}O)_2$-Tc^{IV} core is observed in the XANES and EXAFS studies. See **Tables 3**, **4** and **5**.

Figure 5. EXAFS spectra (left) and Fourier transforms (right) for **$Tc^{V}O$-α1** (a,b) **$Tc^{V}O$-α2** (c) taken at SSRL beamlines 11-2 (a) and 2-3 (b,c). Data are shown in color and fits are given in black. The **$Tc^{V}O$-α1** and **$Tc^{V}O$-α2** samples are from the non-optimized syntheses, where the carryover of the Tc^{IV}-$(\mu\text{-}O)_2$-Tc^{IV} core is observed in the XANES and EXAFS studies. See **Tables 3**, **4** and **5**.

Figure 6. XANES spectrum and fit for sample 115 K (top) and 115 E (bottom).

Figure 7. Technetium speciation in samples as a function of ethyleneglycol content and precipitant used.

Figure 8. General strategy for photolytic reduction of TcO_4^- by α_2-$[P_2W_{17}O_{61}]^{10-}$. The α_2-$[P_2W_{17}O_{61}]^{10-}$ POM (white polyhedra) is promoted to an excited state by irradiation whereupon the excited POM is reduced by 2 electrons by a sacrificial electron donor to the "reduced" α_2-$[P_2W_{17}O_{61}]^{12-}$ (blue polyhedra). The reduced α_2-$[P_2W_{17}O_{61}]^{12-}$ transfers electrons to TcO_4^- resulting in reduction to low valent Tc that will be incorporated into the lacunary POM as the Tc^{V}=O species (red octahedron). The reaction was monitored by ^{31}P NMR: at 12 hours significant amounts of the α_2-$[P_2W_{17}O_{61}]^{10-}$ ligand and intermediate are present. At 24 hr, the **TcO-α2** product is formed in high yield.

Figure 9. ^{31}P NMR of the TBA TcO-α2 product that is formed via the photolytic reduction of TcO_4^- by α_2-$[P_2W_{17}O_{61}]^{10-}$ after 24 hr, followed by isolation as a TBA salt.

Figures for synthesis development manuscript:

Figure 1.

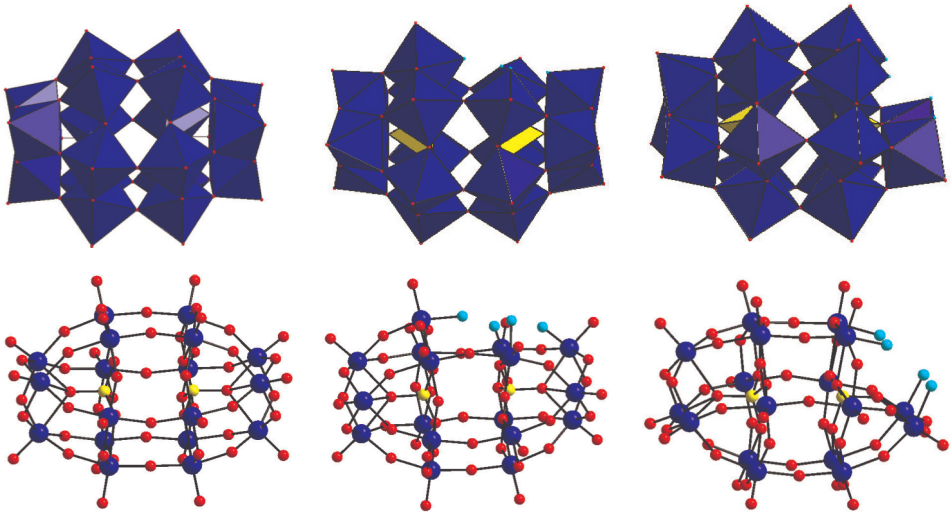

$[\alpha\text{-}P_2W_{18}O_{62}]^{6-}$ $[\alpha_1\text{-}P_2W_{17}O_{61}]^{10-}$ $[\alpha_2\text{-}P_2W_{17}O_{61}]^{10-}$

A **B** **C**

Figure 2.

^{31}P NMR of $Tc^{V}O$-α1 and **$Tc^{V}O$-α2**

Figure 3

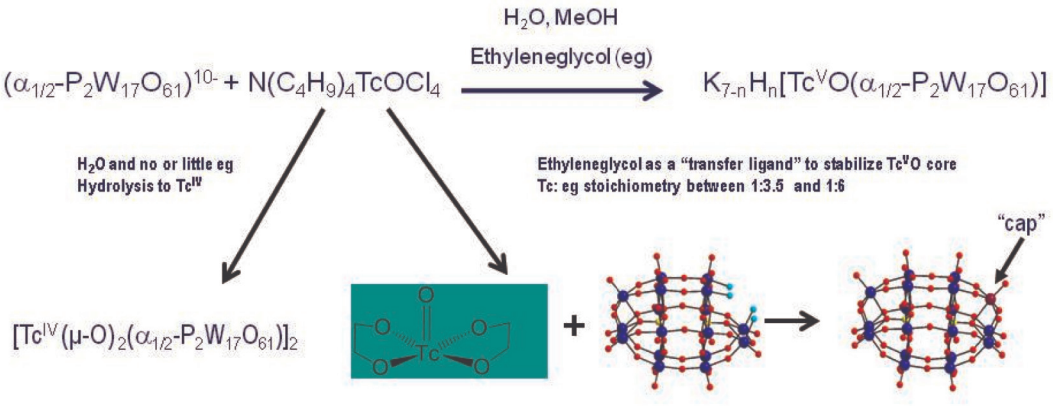

Figure 3. Scheme showing fate of $TcOCl_4^-$ upon hydrolysis to Tc(IV) and upon application of ethyleneglycol as a transfer ligand to preserve the Tc^V=O core for substitution with the POM.

Figure 4. XANES spectra of, from lowest energy to highest energy, $TcO_2 \cdot 2H_2O$ (blue), **$Tc^{V}O$-α2** (red), **$Tc^{V}O$-α1** (black), and TcO_4^- (green). The **$Tc^{V}O$-α1** and **$Tc^{V}O$-α2** samples are from the non-optimized syntheses, where the carryover of the Tc^{IV}-(μ-O)$_2$-Tc^{IV} core is observed in the XANES and EXAFS studies. See **Tables 3**, **4** and **5**.

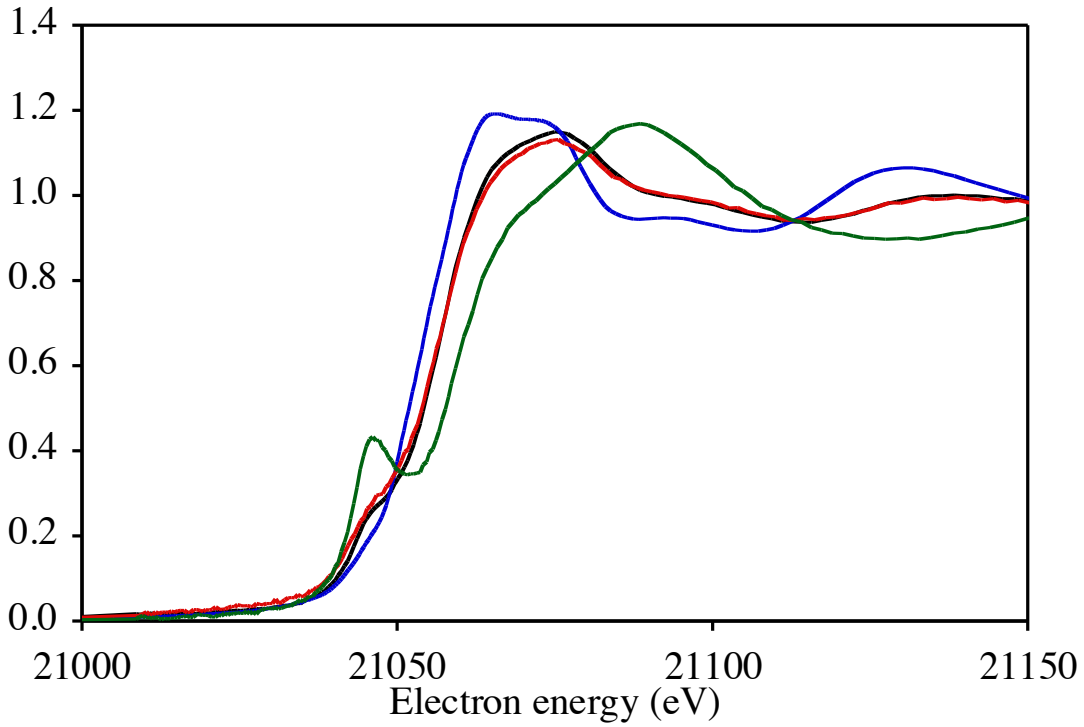

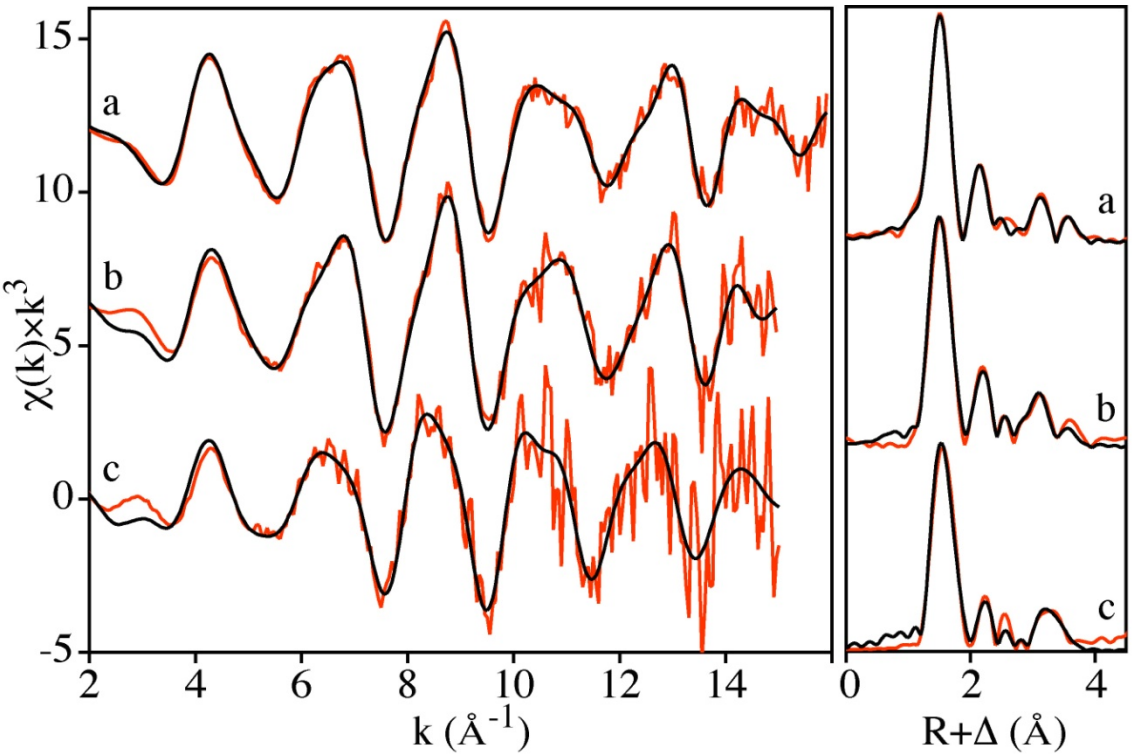

Figure 5. EXAFS spectra (left) and Fourier transforms (right) for **$Tc^{V}O$-α1** (a,b) **$Tc^{V}O$-α2** (c) taken at SSRL beamlines 11-2 (a) and 2-3 (b,c). Data are shown in color and fits are given in black. The **$Tc^{V}O$-α1** and **$Tc^{V}O$-α2** samples are from the non-optimized syntheses, where the carryover of the Tc^{IV}-(μ-O)$_2$-Tc^{IV} core is observed in the XANES and EXAFS studies. See **Tables 3**, **4** and **5**.

Figure 6. XANES spectrum and fit for sample 115 K (top) and 115 E (bottom).

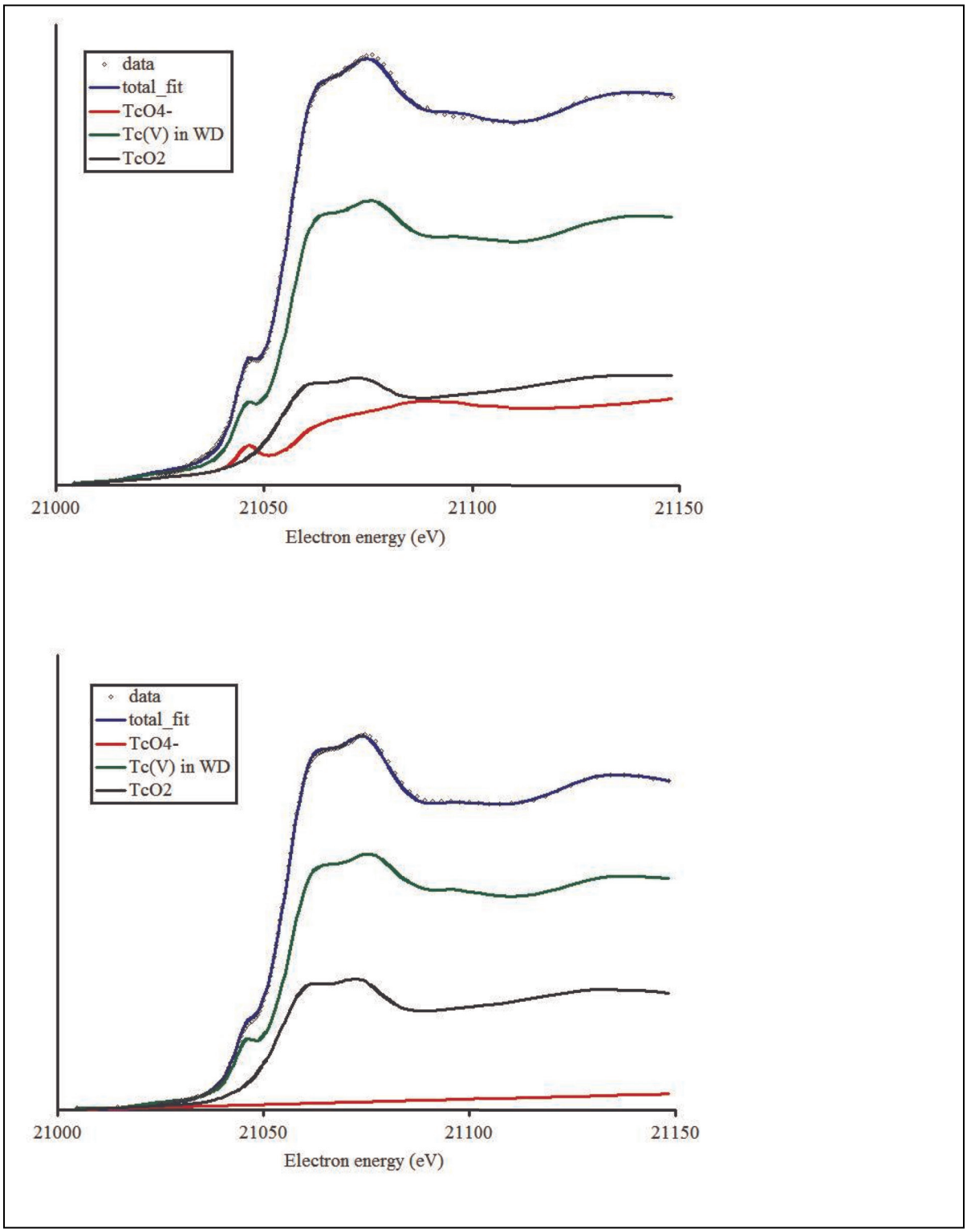

Figure 7. Technetium speciation in samples as a function of ethyleneglycol content and precipitant used.

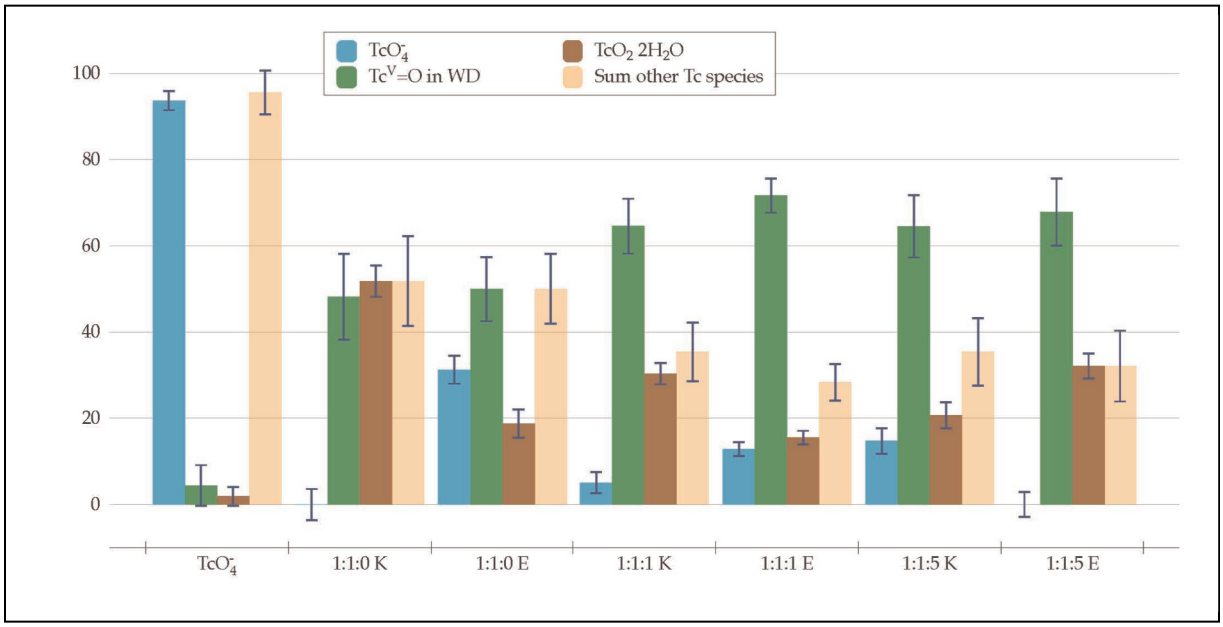

I think we can simplify this diagram to show only TcV alpha 2, ant TcO2 and TcO4- - I think the sum is confusing.

Figure 8. General strategy for photolytic reduction of TcO_4^- by α_2-$[P_2W_{17}O_{61}]^{10-}$. The α_2-$[P_2W_{17}O_{61}]^{10-}$ POM (white polyhedra) is promoted to an excited state by irradiation whereupon the excited POM is reduced by 2 electrons by a sacrificial electron donor to the "reduced" α_2-$[P_2W_{17}O_{61}]^{12-}$ (blue polyhedra). The reduced α_2-$[P_2W_{17}O_{61}]^{12-}$ transfers electrons to TcO_4^- resulting in reduction to low valent Tc that will be incorporated into the lacunary POM as the Tc^V=O species (red octahedron). The reaction was monitored by ^{31}P NMR: at 12 hours significant amounts of the α_2-$[P_2W_{17}O_{61}]^{10-}$ ligand and intermediate are present. At 24 hr, the **TcO-α2** product is formed in high yield.

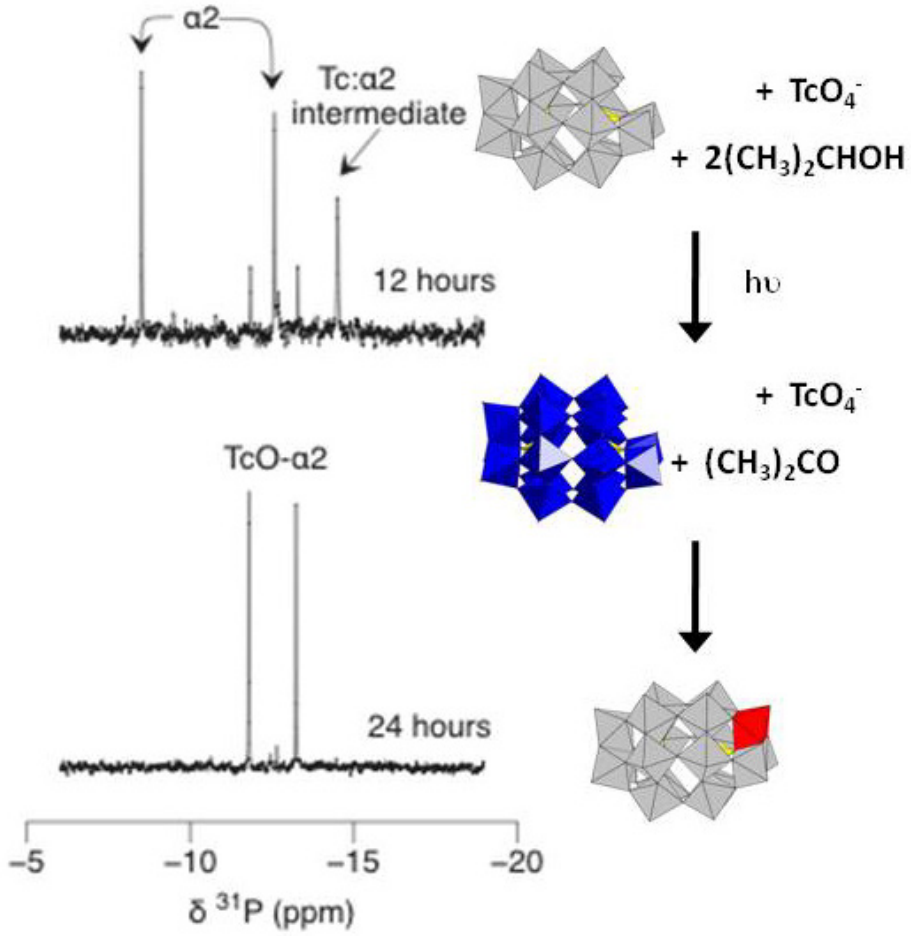

Figure 9. ^{31}P NMR of the TBA TcO-α2 product that is formed via the photolytic reduction of TcO_4^- by α_2-$[P_2W_{17}O_{61}]^{10-}$ after 24 hr, followed by isolation as a TBA salt.

Need picture of NMR here

Tables for Synthesis Development paper

Table 1. Composition of samples for XANES experiments designed to probe speciation of **$Tc^{V}O$-α2**, Tc^{IV}-(μ-O)$_2$-Tc^{IV}, and TcO4- in samples with varying ethyleneglycol. **α2**: α2-$[P_2W_{17}O_{61}]^{10-}$, eg: ethyleneglycol; $TcOCl_4$: TBA $TcOCl_4$

Sample label		***$TcOCl_4$***	***eg***	**α2**	***Precipitant***
110E	Control	1	0	1	EtOH
110 K	Control	1	0	1	KCl
11Eg E	Control	Tc eg complex[1]		1	EtOH
11Eg K	Control	Tc eg complex		1	KCl
115K	Sample	1	5	1	KCl
115E	Sample	1	5	1	EtOH
111K	Sample	1	1	1	KCl
111E	sample	1	1	1	EtOH

[1] $NaTc(eg)_2$ complex used in reaction

Table 2. ^{31}P NMR data showing chemical shifts at various stages of the synthesis of K_7-$nH_n[TcO(\alpha_2$-$P_2W_{17}O_{61})]$ (**$Tc^{V}O$-α2**)

Compound or step in synthesis	**^{31}P NMR shift (ppm)**
Pure K_7-$nH_n[Tc^{V}O(\alpha_2$-$P_2W_{17}O_{61})]$	**-11.60, -13.11**
Crude Rxn mix	No Peaks
Brown Supernatant	**-11.60, -13.11** (-7.75)
Brown Filtrate	**-11.60**, **-13.11**

Table 3: Best fit parameters for the EXAFS spectrum for $Tc^{V}O$-α1 shown in Figure S4a[a]. These data demonstrate the carryover of the Tc^{IV}-(μ-O)$_2$-Tc^{IV} core for "non-optimized" syntheses of **$Tc^{V}O$-α1**. This core occurs due to hydrolysis, when too little ethyleneglycol is used to stabilize the $Tc^{V}O$ starting reagent.

Neighboring Atom	# of Neighbors	σ^2 (Å^2)	Distance (Å)	Distance by Crystallography (Å)[b]	F-Test[c] (p)
O	0.71(3)	0.0032(6)	1.705(5)	1.72	1×10^{-6}
O	4	0.0050(2)	1.975(4)	1.88-1.96	4×10^{-13}
O	1	0.010(4)	2.42(3)	2.34	0.08
Tc	0.29(3)	0.003[d]	2.531(5)		6×10^{-6}
W[e]	1			3.37	
P	1	0.0024(7)	3.463(9)	3.51	2×10^{-4}
W	3	0.008(1)	3.75(1)	3.69-3.75	0.01
O	4	0.005(1)	3.84(1)	3.69-3.88	1×10^{-3}

a) Fit range: 2<k<16, 0.8<R<4; 28 independent data. 15 parameters, 0.12 Å resolution, $S_0^2 = 1$, $\Delta E_0 = -15(1)$ eV, $\chi^2 = 80$, $\chi_\nu^2 = 6.1$, R = 0.01.
b) Dawson, B. Acta. Cryst. 1953, 6, 113 – 126.
c) F-test determines the significance of the improvement to the fit created by adding an additional set of atoms. If the p-value is less than 0.05, the additional atoms have significantly improved the fit and can be considered "observed" in the EXAFS experiment.
d) Debye-Waller of Tc shell fixed to allow comparison between samples.
e) Inclusion of this shell did not improve fit to data

Table 4: Best fit parameters for Tc(α_1 $P_2W_{17}O_{61}$)[a] taken at SSRL beamline 2-3, shown in **Figure 4B**. These data demonstrate the carryover of the Tc^{IV}-(μ-O)$_2$-Tc^{IV} core for "non-optimized" syntheses of **Tc^{V}O-α1**. This core occurs due to hydrolysis, when too little ethyleneglycol is used to stabilize the Tc^{V}O starting reagent.

Neighboring Atom	# of Neighbors	σ^2 (Å^2)	Distance (Å)	Distance by Crystallography (Å)	Hamilton Test[b] (p)
O	0.72(3)	0.0021(6)	1.694(5)	1.72	6×10^{-6}
O	4[c]	0.0049(3)	1.985(6)	1.88-1.96	3×10^{-9}
O	1	0.011(5)	2.32(3)	2.34	0.04
Tc	0.28(3)	0.003[d]	2.555(7)		9×10^{-5}
W[e]	1			3.37	
P	1	0.0011(6)	3.474(6)	3.51	3×10^{-4}
W	3	0.012(2)	3.75(2)	3.69-3.75	0.06
O[e]	4			3.69-3.88	

a) Fit range: $2<k<15$, $1<R<4$, 24.5 independent data. 14 parameters, 0.13 Å resolution, $S_0^2 = 1$, $\Delta E_0 = -11(2)$ eV, $\chi^2 = 46.7$, $\chi_\nu^2 = 4.4$, $R = 0.01$.
b) Hamilton test determines the significance of the improvement to the fit created by adding an additional set of atoms. If the p-value is less than 0.05, the additional atoms have significantly improved the fit and can be considered "observed" in the EXAFS experiment.
c) Multiple scattering from the *trans* oxygen ligands is also included at twice the bond distance
d) Debye-Waller of Tc shell fixed to allow comparison between samples.
e) Inclusion of this shell did not improve fit to data

Table 5: Best fit parameters for the EXAFS spectrum for K^+ salt of $Tc^{V}O$-α2 shown in Figure 4c[a]. These data demonstrate the carryover of the Tc^{IV}-(μ-O)$_2$-Tc^{IV} core for "non-optimized" syntheses of **$Tc^{V}O$-α2**. This core occurs due to hydrolysis, when too little ethyleneglycol is used to stabilize the $Tc^{V}O$ starting reagent.

Neighboring Atom	# of Neighbors	σ^2 (Å^2)	Distance (Å)	Distance by Crystallography[b] (Å)	F Test[c] (p)
O	0.84(4)	0.0024(6)	1.736(5)	1.71	2×10^{-5}
O	4[d]	0.0040(3)	2.008(7)	1.85-1.92	2×10^{-8}
O	1	0.007(3)	2.31(2)	2.33	0.01
Tc	0.16(4)	0.003[e]	2.57(1)		7×10^{-3}
W	2	0.0093(8)	3.35(2)	3.37	0.01
P[f]	1			3.52	
W	2	0.0093[g]	3.89(2)	3.70-3.72	0.06
O[f]	4			3.72-3.83	

a) Fit range: 2<k<15, 1.1<R<3.9, 24 independent data. 13 parameters, 0.13 Å resolution, $S_0^2 = 1$, $\Delta E_0 = -11(2)$ eV, $\chi^2 = 15$, $\chi_\nu^2 = 1.5$, R = 0.02.
b) Dawson, B. Acta. Cryst. 1953, 6, 113 – 126.
c) F-test determines the significance of the improvement to the fit created by adding an additional set of atoms. If the p-value is less than 0.05, the additional atoms have significantly improved the fit and can be considered "observed" in the EXAFS experiment.
d) Multiple scattering from the *trans* oxygen ligands is also included at twice the bond distance
e) Debye-Waller factor of Tc shell fixed to allow comparison between samples.
f) Inclusion of this shell did not improve fit to data
g) Debye-Waller factor of second set of W atoms constrained to equal that of the first set of W atoms.

Table 6: Tc speciation in reactions performed as a function of ethyleneglycol and precipitant [a]

Sample	α2:Tc:eg	Isolation method	TcO_4^-	$Tc^VO\alpha2$	$TcO_2 \cdot 2H_2O$
TcO_4^-	-	-	0.94(2)	0.04(5)	0.02(3)
11 Eg E[b]	1:1-1	ethanol	0.24(7)	0.1(2)	0.6(1)
110K	1:1:0	KCl	0.00(4)	0.5(1)	0.52(7)
110E	1:1:0	ethanol	0.31(3)	0.50(7)	0.19(5)
111K	1:1:1	KCl	0.05(2)	0.65(6)	0.30(4)
111E	1:1:1	ethanol	0.13(2)	0.72(4)	0.16(4)
115K	1:1:5	KCl	0.15(3)	0.65(7)	0.21(5)
115E	1:1:5	ethanol	0.00(3)	0.68(8)	0.32(5)

a) The number in parentheses is the standard deviation in the same units as the last digit in the number (e.g., 0.17(1) is 0.17 with a standard deviation of 0.01).

b) This is a sample prepared from 1:1 $Tc(eg)_2$- complex: α2 ligand.

REFERENCES

(1) Burke, I. T.; Boothman, C.; Lloyd, J. R.; Livens, F. R.; Charnock, J. M.; McBeth, J. M.; Mortimer, R. J. G.; Morris, K. *Environ. Sci. Technol.* 2006, *40*, 3529.

(2) Burke, I. T.; Boothman, C.; Lloyd, J. R.; Mortimer, R. J. G.; Livens, F. R.; Morris, K. *Environ. Sci. Technol.* 2005, *39*, 4109.

(3) Istok, J. D.; Senko, J. M.; Krumholz, L. R.; Watson, D.; Bogle, M. A.; Peacock, A.; Chang, Y. J.; White, D. C. *Environ. Sci. Technol.* 2004, *38*, 468.

(4) Lukens, W. W.; Bucher, J. J.; Shuh, D. K.; Edelstein, N. M. *Environ. Sci. Technol.* 2005, *39*, 8064.

(5) Lukens, W. W.; Shuh, D. K.; Schroeder, N. C.; Ashley, K. R. *Environ. Sci. Technol.* 2004, *38*, 229.

(6) Maes, A.; Geraedts, K.; Bruggeman, C.; Vancluysen, J.; Rossberg, A.; Henning, C. *Environ. Sci. Technol.* 2004, *38*, 2044.

(7) Stalmans, M.; Maes, A.; Cremers, A. In *Technetium in the Environment*; Desmet, G., Myttenaere, C., Eds.; Elsevier, Appl. Sci. Publ.: 1986, p 91.

(8) Wildung, R. E.; Li, S. W.; Murray, C. J.; Krupka, K. M.; Xie, Y.; Hess, N. J.; Roden, E. E. *FEMS Microbiology Ecology* 2004, *49*, 151.

(9) Beals, D. M.; Hayes, D. W. *Science of the Total Environment* 1995, *173*, 101.

(10) Hunt, A. G.; Skinner, T. E. *Hydrogeology Journal* 2010, *18*, 381.

(11) U.S. Department of Energy, O. o. B. E. S.; http://www.sc.doe.gov/bes/reports/files/ANES_rpt.pdf: 2006; Vol. 2006.

(12) Burton-Pye, B. P.; Radivojevic, I.; McGregor, D.; Mbomekalle, I. M.; Lukens, W. W., Jr.; Francesconi, L. C. *J. Amer. Chem. Soc.* 2011, *133*, 18802.

(13) McGregor, D.; Burton-Pye, B. P.; Howell, R. C.; Mbomekalle, I. M.; Lukens, W. W.; Bian, F.; Mausolf, E.; Poineau, F.; Czerwinski, K. R.; Francesconi, L. C. *Inorg. Chem. (Washington, DC, U. S.)* 2011, *50*, 1670.

(14) Burton-Pye, B. P.; McGregor, D.; Lukens, W. W., Jr.; Francesconi, L. C. *manuscript in preparation* 2012.

(15) Keita, B.; Girard, F.; Nadjo, L.; Contant, R.; Canny, J.; Richet, M. *Journ. of Electroanal. Chem.* 1999, *478*, 76.

(16) Keita, B.; Levy, B.; Nadjo, L.; Contant, R. *New. J. Chem.* 2002, *26*, 1314.

(17) Keita, B.; Mbomekalle, I.-M.; Nadjo, L.; Contant, R. *Eur. J. Inorg. Chem.* 2002, 473.

(18) Davison, A.; Trop, H.; DePamphilis, B.; Jones, A. *Inorganic Synthesis* 1982, *21*, 160.

(19) Contant, R. *Inorg. Synth.* 1990, *27*, 71.

(20) Ciabrini, J.-P.; Contant, R. *J. Chem. Research (M).* 1993, 2720.

(21) Venturelli, A.; Nilges, M. J.; Smirnov, A.; Belford, R. L.; Francesconi, L. C. *J. Chem. Soc., Dalton Trans.* 1999, 301.

(22) Newville, M. J. *Synchrotron Rad.* 2001, *8*, 322.

(23) Ravel, B. *Physica Scripta* 2005, *T115*, 1007.

(24) Rehr, J. J.; Albers, R. C.; Zabinsky, S. I. *Phys. Rev. Lett.* 1992, *69*, 3397.

(25) D'Amour, V. H. *Acta Cryst.* 1976, *B32*, 729.

(26) Bevington, P. R.; Robinson, K. D. *Data Reduction and Error Analysis for the Physical Sciences*; McGraw-Hill: Boston, MA, 1992.

(27) Downward, L.; Booth, C. H.; Lukens, W. W.; Bridges, F. In *AIP Conference Proceedings* 2007; Vol. 882, p 129.

(28) Davison, A.; DePamphilis, B. V.; Jones, A. G.; Franklin, K. L.; Lock, C. J. L. *Inorg. Chim. Acta* 1987, *128*, 161.

(29) DePamphilis, B. V.; Jones, A. G.; Davison, A. *Inorg. Chem.* 1983, *22*, 2292.

(30) Lloyd, J. R.; Sole, V. A.; Van Praagh, C. V. G.; Lovley, D. R. *Appl. Environ. Microbiol.* 2000, *66*, 3743.

(31) Lukens, J., W.W.; Bucher, J. J.; Edelstein, N. M.; Shuh, D. K. *Environ. Sci. Technol.* 2002, *36*, 1124.

(32) McGregor, D.; Burton-Pye, B. P.; Mbomekalle, I. M.; Aparicio, P. A.; Romo, S.; Lopez, X.; Poblet, J. M.; Francesconi, L. C. *submitted* 2012.

(33) Antonaraki, S.; Triantis, T. M.; Papaconstantinou, E.; Hiskia, A. *Catal. Today* 2010, *151*, 119.

(34) Choi, W. *Prepr. Ext. Abstr. ACS Natl. Meet., Am. Chem. Soc., Div. Environ. Chem.* 2006, *46*, 400.

(35) Ettedgui, J.; Diskin-Posner, Y.; Weiner, L.; Neumann, R. *J. Am. Chem. Soc.* 2011, *133*, 188.

(36) Grika, E.; Troupis, A.; Hiskia, A.; Papaconstantinou, E. *Environ. Sci. Technol.* 2005, *39*, 4242.

(37) Hiskia, A.; Troupis, A.; Antonaraki, S.; Gkika, E.; Papaconstantinou, P. K. *Int. J. Environ. Anal. Chem.* 2006, *86*, 233.

(38) Hiskia, A.; Troupis, A.; Papaconstantinou, E. *International Journal of Photoenergy* 2002, *4*, 35.

(39) Jin, H.; Wu, Q.; Pang, W. *J. Hazard. Mater.* 2007, *141*, 123.

(40) Keita, B.; Liu, T.; Nadjo, L. *J. Mater. Chem.* 2009, *19*, 19.

(41) Kormali, P.; Troupis, A.; Triantis, T.; Hiskia, A.; Papaconstantinou, E. *Catal. Today* 2007, *124*, 149.

(42) Liu, L.; Wang, L.-m.; Chu, D.-q. *Adv. Mater. Res. (Zuerich, Switz.)* 2010, *113-116*, 2045.

(43) Mandal, S.; Mandale, A. B.; Sastry, M. *J. Mater. Chem.* 2004, *14*, 2868.

(44) Mandal, S.; Rautaray, D.; Sastry, M. *J. Mater. Chem.* 2003, *13*, 3002.

(45) Troupis, A.; Hiskia, A.; Papaconstantinou, E. *New J. Chem.* 2001, *25*, 361.

(46) Finke, R. G. *Transition Metal Nanoclusters: solution-phase synthesis, then characterization and mechanism of formation, of polyoxoanion-and tetrabutylammonium-stabilized nanoclusters*; Marcel Dekker, Inc: New York, 2001.

(47) Lin, Y.; Finke, R. G. *J. Amer. Chem. Soc.* 1994, *116*, 8335.

(48) Burton-Pye, B. P.; McGregor, D.; Francesconi, L. C. *manuscript in preparation* 2012.

DISCLAIMER